Cooperation between Rb and Arf in suppressing mouse retinoblastoma

Karina Conkrite,[1] Maggie Sundby,[1] David Mu,[2] Shizuo Mukai,[3] and David MacPherson[1]

[1]Department of Embryology, Carnegie Institution, Baltimore, Maryland, USA. [2]Department of Pathology and Department of Biochemistry and Molecular Biology, Pennsylvania State University College of Medicine, Hershey, Pennsylvania, USA. [3]Department of Ophthalmology, Massachusetts Eye and Ear Infirmary, Harvard Medical School, Boston, Massachusetts, USA.

Retinoblastoma is a pediatric cancer that has served as a paradigm for tumor suppressor gene function. Retinoblastoma is initiated by *RB* gene mutations, but the subsequent cooperating mutational events leading to tumorigenesis are poorly characterized. We investigated what these additional genomic alterations might be using human retinoblastoma samples and mouse models. Array-based comparative genomic hybridization studies revealed deletions in the *CDKN2A* locus that include *ARF* and *P16INK4A*, both of which encode tumor suppressor proteins, in both human and mouse retinoblastoma. Through mouse genetic analyses, we found that *Arf* was the critical tumor suppressor gene in the deleted region. In mice, inactivation of one allele of *Arf* cooperated with *Rb* and *p107* loss to rapidly accelerate retinoblastoma, with frequent loss of heterozygosity (LOH) at the *Arf* locus. Arf has been reported to exhibit p53-independent tumor suppressor roles in other systems; however, our results showed no additive effect of *p53* and *Arf* coinactivation in promoting retinoblastoma. Moreover, *p53* inactivation completely eliminated any selection for *Arf* LOH. Thus, our data reveal important insights into the p53 pathway in retinoblastoma and show that Arf is a key collaborator with Rb in retinoblastoma suppression.

Introduction

Human retinoblastoma is initiated by mutation of both alleles of *RB*, but other changes are required for malignancy (1, 2). RB is a central regulator of proliferation that acts to inhibit E2F transcription factors through direct inhibition and through recruitment of chromatin-modifying enzymes (3). Recent evidence suggests that human retinoblastoma may be derived from a benign lesion, retinoma, caused by *RB* inactivation (4). Indeed, nonproliferative retinoma, but not retinoblastoma, was correlated with high levels of the RB family member p130, suggesting that, in the absence of RB, other family members can enforce cell cycle exit and inhibit tumorigenesis (4). Studies of retinoma using human samples are limited in that retinomas can only be examined in cases in which late-stage retinoblastoma leads to removal of the eye. Early-stage human retinomas cannot be readily accessed for histological or molecular analyses, making it difficult to know whether retinoma truly represents a precursor lesion to retinoblastoma.

Mouse models based on *Rb* deletion can provide insight into tumor origins and progression. Loss of *Rb* and *p107* leads to retinoblastoma that arises with long latency and incomplete penetrance (5, 6). Examination of secondary alterations may provide insight into the nature of the switch to malignant retinoblastoma. Human retinoblastomas exhibit consistent regions of chromosomal alteration, including 6p and 1q gains, suggesting that *RB* loss may not be sufficient for human retinoblastoma (1, 2). Several candidate genes have been described. For example, *NMYC* is amplified in human and murine retinoblastoma (1, 2, 6). The p53 pathway may also play a role in human retinoblastoma. One study reported that the p53 pathway is evaded through amplifications in *MDM4* (7). Another found *MDM2* to be highly expressed (8). The latter study suggested that intrinsically high *MDM2* levels synergize with *RB* loss in promoting retinoblastoma. It has also been reported that *Arf* is highly expressed in human retinoblastoma (7). This is consistent with *Arf* being an E2F target gene that would be expected to be deregulated upon *RB* inactivation (9, 10). Whether *Arf* has any functional role in retinoblastoma suppression is unknown. Efforts are being undertaken to develop activators of the p53 pathway as potential treatment for retinoblastoma (7, 11). However, the importance of this pathway for retinoblastoma is unclear. In this study, we use genomic analyses and mouse genetics to explore roles for Arf and for other p53 pathway components in retinoblastoma.

Results

Human retinoblastoma has been proposed to arise from benign retinoma (4). We studied a mouse model of retinoblastoma initiated by retina-specific *Rb* deletion on a background of a null mutation in the *Rb*-related gene *p107*. In this model, *Cre* is expressed in the mid-periphery to far-periphery of the retina through the use of the *Pax6* α enhancer *Cre* transgenic allele (12), and retinoblastoma arises with partial penetrance and long latency (6). *Rb* and *p107* loss during development of the retina leads extensive cell death prior to detection of retinoblastoma, although certain cell types survive *Rb/p107* deletion (5, 6, 13). We examined $Rb^{lox/lox}$;$p107^{-/-}$;*Pax6* α *Cre* (*Rb/p107DKO*) retinas from mice that did not develop retinoblastoma to determine whether premalignant lesions could be detected. As Sox2 and syntaxin mark the vast majority of murine retinoblastoma cells (14), we stained for these markers in *Rb/p107DKO* retinas at 1 year of age. In addition to observing retinal degeneration, we also detected the presence of nonproliferative lesions that resembled retinoblastoma based on Sox2/syntaxin expression (Supplemental Figure 1; supplemental material available online with this article; doi:10.1172/JCI61403DS1). These observations suggest that a cell cycle block may form a barrier to murine reti-

Conflict of interest: The authors have declared that no conflict of interest exists.
Citation for this article: *J Clin Invest.* 2012;122(5):1726–1733. doi:10.1172/JCI61403.

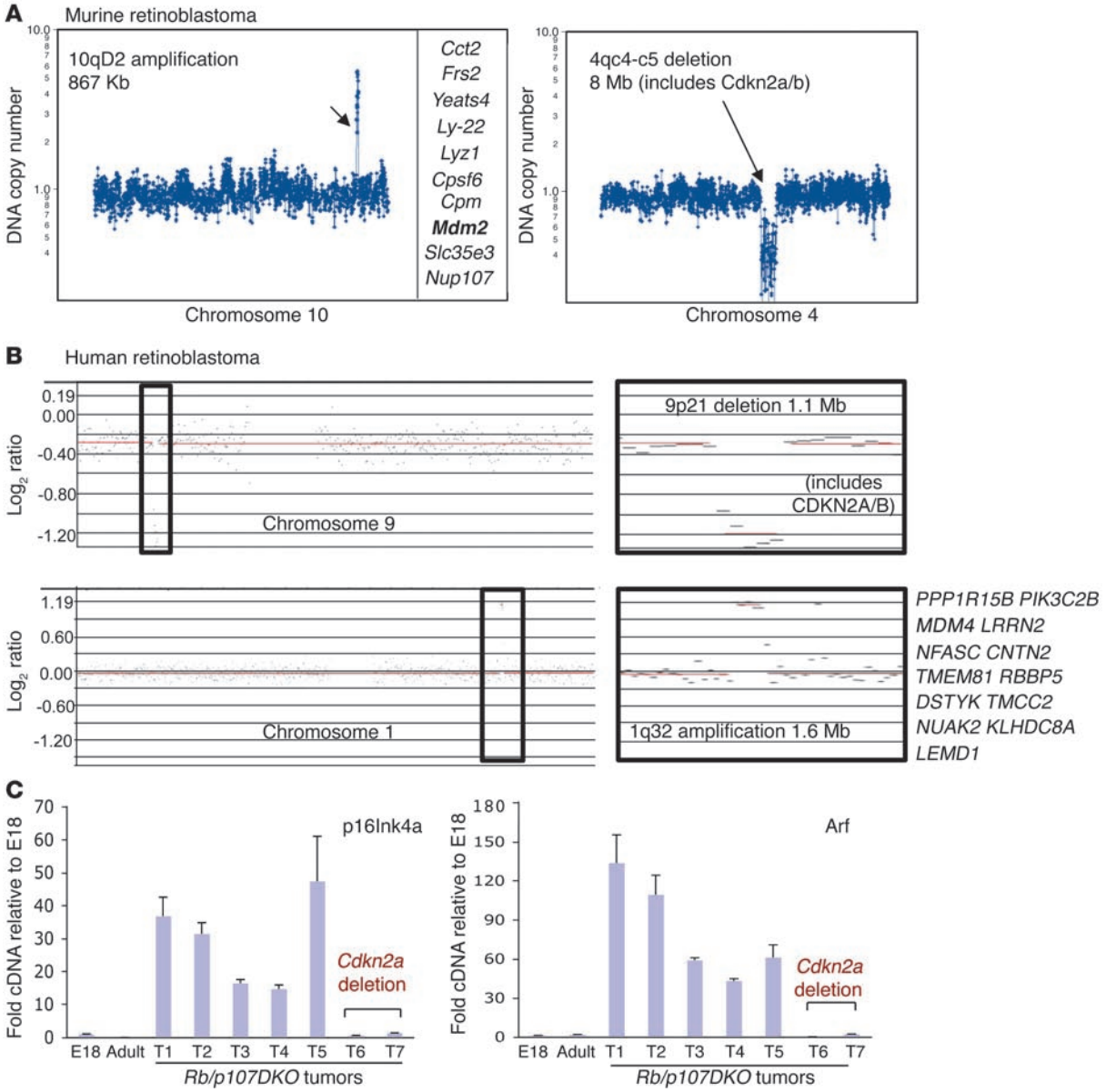

Figure 1

CDKN2A/*Cdkn2a* deletions in retinoblastoma. (**A**) Array-CGH analyses of *Rb*/*p107DKO* retinoblastomas with 10qD2 amplifications that include *Mdm2* (arrow indicates region of amplification) and 4qC4-5 deletions that include *p16*/*Arf* (arrow indicates region of deletion). RefSeq genes in 10qD2 amplicon are shown. (**B**) Array-CGH analyses of human retinoblastomas showing 9p21 deletion (including *p16*/*ARF*) and 1q32 amplification (including *MDM4*). RefSeq genes within the 1q32 amplicon are shown. (**C**) Real-time PCR showing expression of *p16INK4a* and *Arf* in murine retinoblastomas but not in tumors with homozygous *Cdkn2a* genomic deletions. Tumors (T1) are shown on the *x* axis.

noblastoma, as suggested in human retinoblastoma studies (4). A block to tumorigenesis overcome through secondary mutations may involve suppression of cell death or bypass of a cell cycle arrest. The p53 tumor suppressor has been implicated in both apoptosis and cell cycle arrest but is not directly mutated in human retinoblastoma. To better understand the blocks to tumorigenesis that must be overcome through secondary alterations, we performed genomic analyses.

Array-based comparative genomic hybridization analyses of p53 pathway alterations in murine and human retinoblastoma. Using array-based comparative genomic hybridization (array-CGH) data from 21 *Rb/p107DKO* retinoblastomas, including 14 primary and 7 metastatic tumors, we focused on alterations that might disrupt known p53 pathway components. *MDM4* has been implicated as genetically altered in human retinoblastoma (7). Murine *Mdm4* is located at 1qE4. Of the 21 murine retinoblastomas, no high-level amplifications or focal alterations including *Mdm4* were observed, although gains of the entire chromosome 1 were found in 7 out of 21 murine retinoblastomas. We did observe 1 *Rb/p107DKO* retinoblastoma with a focal *Mdm2* amplification that correlated with high *Mdm2* expression (Figure 1A and Supplemental Figure 2). A previous study indicated

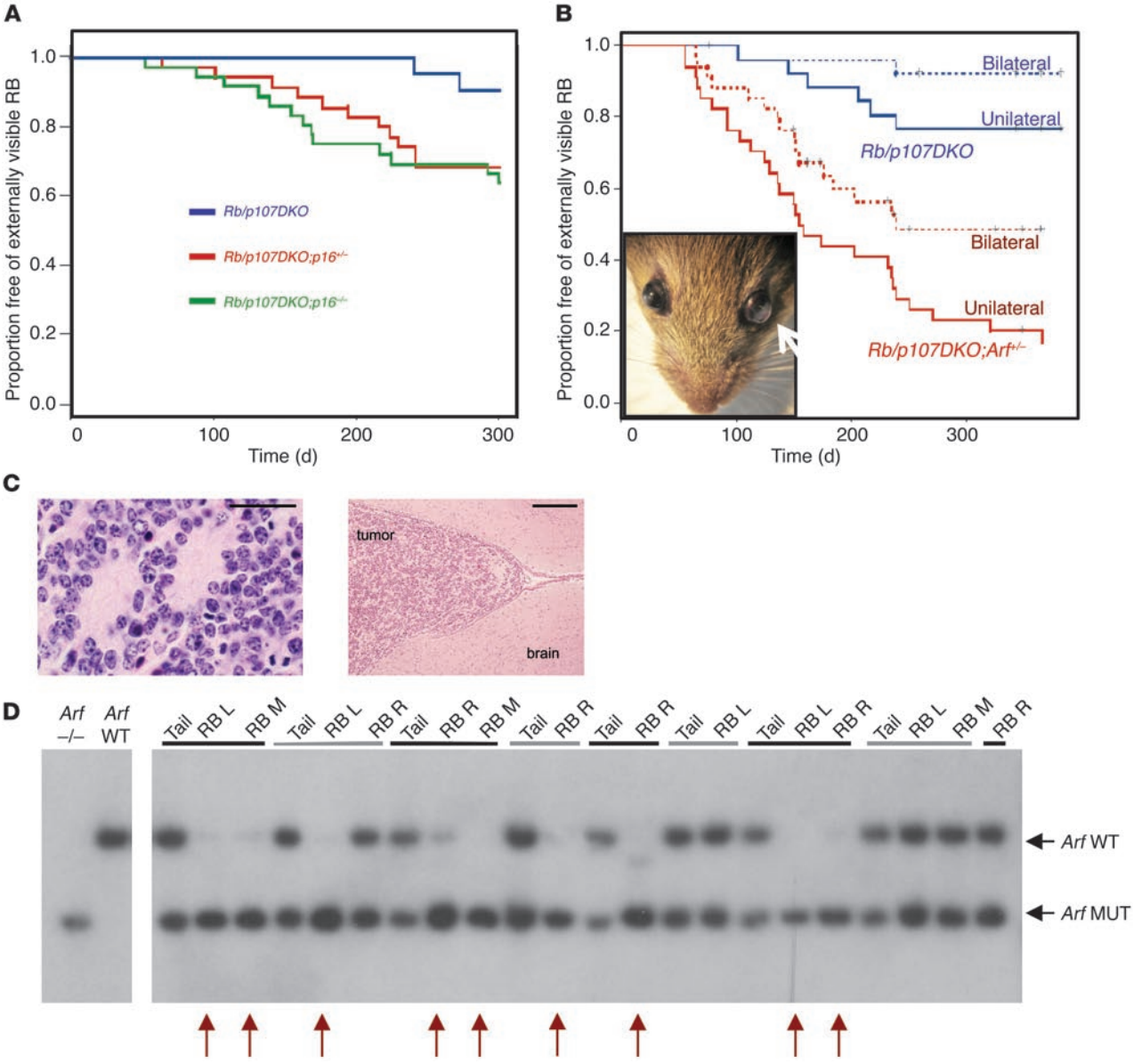

Figure 2

Arf loss promotes murine retinoblastoma. (**A**) Observational curves showing time to first appearance of retinoblastomas (RBs) in the anterior chamber of the eyes for *Rb/p107DKO*, *Rb/p107DKO;p16*$^{+/-}$, and *Rb/p107DKO;p16*$^{-/-}$ mice. (**B**) Similar curves for *Rb/p107DKO* mice compared with those for *Rb/p107DKO;Arf*$^{+/-}$ mice. Here, mice were also followed for bilateral retinoblastoma (dashed lines). The inset shows the gross image of an eye a from *Rb/p107DKO;Arf*$^{+/-}$ mouse, showing a tumor with anterior chamber invasion (arrow). (**C**) H&E image of histological appearance of *Rb/p107DKO;Arf*$^{+/-}$ retinoblastoma (left) and brain metastasis (right). Scale bar: 30 μm (left); 100 μm (right). (**D**) Southern blot showing LOH for *Arf* in a subset of *Rb/p107DKO;Arf*$^{+/-}$ mice (red arrows). Tumors from the left eye (L) and right eye (R) or metastasis (M) are indicated, along with tail DNA from the same animal.

that 65% of human retinoblastomas exhibit increased *MDM4* copy number (7). However, that study did not define the size of the region of amplification. We examined *MDM4* copy number alterations in human retinoblastoma samples using array-CGH. Out of 37 human retinoblastomas, 2 exhibited focal amplifications (1.6 Mb, 9.2 Mb) (Figure 1B). In addition, 17 out of 37 retinoblastomas exhibited gain of the long arm of 1q, which included *MDM4* at 1q32 (Supplemental Figure 3). Thus, both human and murine retinoblastomas exhibited large regions of chromosomal gain that included *MDM4*, and a small subset (2 out of 37) of human retinoblastomas exhibited high-level focal *MDM4* amplification.

CDKN2A deletions in a subset of murine and human retinoblastomas. Thus far unexplored in genetic analyses of retinoblastoma, the MDM2 inhibitor Arf is an activator of the p53 pathway. Our genomic analyses of murine retinoblastoma revealed the occurrence of recurrent 4qC4-5 deletions in 3 out of 21 *Rb/p107DKO* retinoblastomas (Figure 1A). The deletion included the *Cdkn2a* locus, encoding both *p16INK4a* and *Arf* (15). Both bona fide tumor suppressors, *p16INK4a* and *Arf* have different promoters

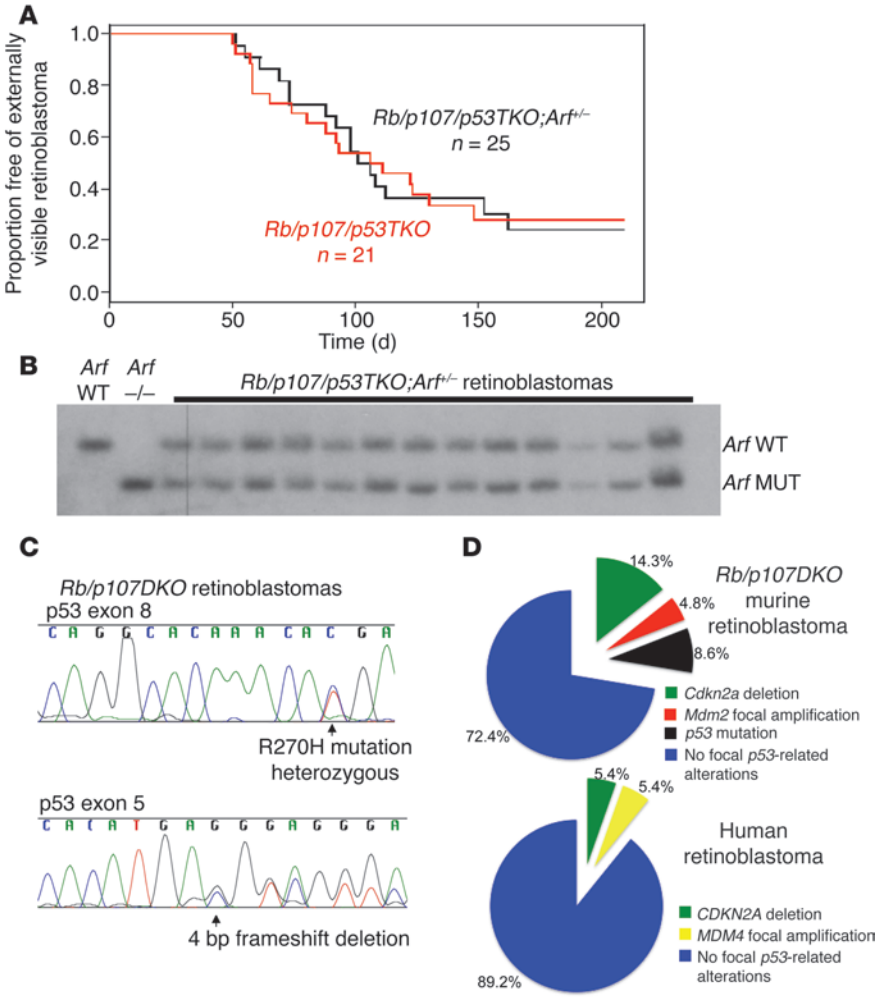

Figure 3

Inactivation of *p53* abrogates selection for *Arf* LOH in murine retinoblastoma. (**A**) Observational curves showing time to first appearance of retinoblastomas in the anterior chamber of the eyes of *Rb/p107/p53TKO* mice and *Rb/p107/p53TKO;Arf*$^{+/-}$ mice. (**B**) Southern blot analysis showing that 0 out of 13 *Rb/p107/p53TKO;Arf*$^{+/-}$ retinoblastomas exhibit LOH for *Arf*. (**C**) Sequencing traces showing direct p53 mutation in a subset of murine retinoblastomas from *Rb/p107DKO* animals. (**D**) Pie charts showing the frequency of *p53*-related focal genetic alterations in murine *Rb/p107DKO* and human retinoblastoma. Charts do not include whole chromosome or chromosome arm gains or losses.

and first exons but share exons 2 and 3, translated using differing reading frames (15). The minimal deleted region across 3 tumors was 7.5 Mb. Real-time PCR analyses showed that 2 out of the 3 deletions were homozygous, while the third was consistent with a hemizygous mutation or of a mixed oligoclonal tumor (Supplemental Figure 4A). We also used real-time PCR to confirm that both p16 and Arf are expressed in tumors that did not harbor 4qc4-5 deletion (Figure 1C). We examined human retinoblastomas for alterations in *CDKN2A*. Array-CGH revealed that 2 out of 37 human retinoblastomas exhibited focal deletions at *CDKN2A* (1.1 Mb and 3.3 Mb) (Figure 1B). Notably, when considering the minimal region of common deletion across both mouse and human retinoblastoma, the only commonly deleted genes were *Mtap*, *Cdkn2a* (encoding *p16INK4a* and *Arf*), and *Cdkn2b*. We focused analyses on *p16INK4a* and *Arf*. *p16INK4a* functions upstream of the entire RB family, RB, p107, and p130 as a CDK inhibitor. If *p16INK4a* were the critical gene in the deleted region, this would suggest that even in the absence of pRB and p107, selection for regulators of p130 activity may be important. If *Arf* were the critical gene, this would implicate another component of the *p53* pathway beyond *MDM2/MDM4* as being important for retinoblastoma or might indicate *p53*-independent effects. We sequenced exons 1α and 1β as well as exon 2 of the *Cdkn2a* locus in 19 mouse retinoblastomas and 37 human retinoblastomas to determine whether either *p16* or *Arf* are inactivated through subtle mutations. In analyses of both human and murine primary retinoblastomas, no *p16/Arf* point mutations or indels were detected. Thus, as in many tumor types (16), *p16/Arf* inactivation in retinoblastoma occurred through large deletions without subtle mutations.

Mouse genetic analysis of Cdnk2a locus in retinoblastoma. We proceeded with mouse genetic analyses to assess whether either *p16INK4a* or *Arf* were important retinoblastoma suppressors. We performed compound mutant analyses using the *Rb/p107/DKO* model. We generated *Rb/p107DKO;p16*$^{+/+}$, *Rb/p107DKO;p16*$^{+/-}$, and *Rb/p107DKO;p16*$^{-/-}$ cohorts and followed mice for tumor development. Mice were monitored for first appearance of externally visible retinoblastoma in the anterior chamber of the eye. When retinoblastoma was initiated by loss of both *Rb* and *p107*, inactivation of either one or both alleles of *p16* led to a rather modest acceleration of late-stage tumorigenesis (Figure 2A). Over 300 days, 2 out of 22 (9%) *Rb/p107DKO* control mice, compared with 12 out of 32 (38%) *Rb/p107DKO;p16*$^{+/-}$ animals and 14 out of 36 (39%) *Rb/p107DKO;p16*$^{-/-}$ animals developed retinoblastoma with anterior chamber invasion. Of the mice that developed retinoblastoma, the average time to visible tumor was 255 days in *Rb/p107DKO* controls, 185 days in *Rb/p107DKO;p16*$^{+/-}$ cohorts, and 179 days in *Rb/p107DKO;p16*$^{-/-}$ cohorts. The effect of p16 loss in promoting retinoblastoma is much weaker than that of strong *Rb/p107* cooperating mutations, such as *p53* deletion or the microRNA *miR-17-92* overexpression, previously reported (7, 14). Nonetheless, the mild retinoblastoma-promoting effect of *p16INK4a* deletion supports the notion that CDK inhibitors can exhibit tumor suppressor function in retinoblastoma (14, 17).

Arf is a potent retinoblastoma suppressor in mouse models. We also examined the role of *Arf* in retinoblastoma suppression using the *Rb/p107DKO* model. We note that *Arf*-null mice exhibit failure in regression of the hyaloid vessels that are normally transiently present during eye development (18). The *Arf*$^{-/-}$ defect

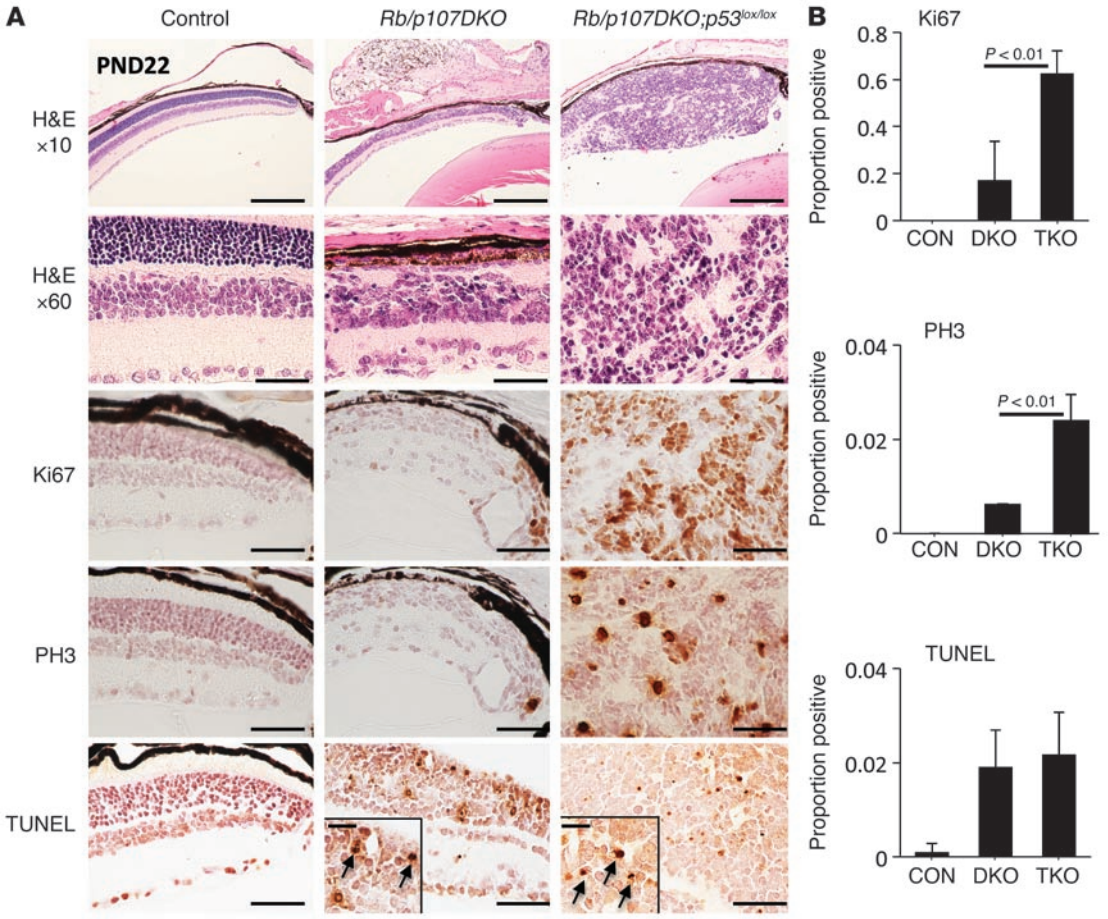

Figure 4

Inactivation of *p53* increases proliferation in the *Rb/p107DKO* retina without suppressing cell death. (**A**) Histology, Ki67 and phospho-histone H3 (PH3) immunostaining and TUNEL analyses showing retinal phenotypes of the following genotypes: *Cre*-negative control, *Rb/p107DKO*, and *Rb/p107DKO;p53*$^{lox/lox}$. Arrows indicate TUNEL positive nuclei. Scale bar: 270 μm (first row); 50 μm (second, third, fourth, and bottom rows); 20 μm (TUNEL insets). (**B**) Quantification of Ki67, phospho-histone H3, and TUNEL data. n = 4–5 animals per data point. CON, control; DKO, *Rb/p107DKO*; TKO, *Rb/p107/p53TKO*. Error bars refer to standard deviation. P values shown are from Student's t test.

leads to secondary degeneration of the retina and complicates analyses of *Arf* homozygous animals. Since *Arf* heterozygote mice exhibit normal hyaloid regression (18), we compared *Rb/p107DKO;Arf*$^{+/+}$ cohorts with *Rb/p107DKO;Arf*$^{+/-}$ cohorts and followed them for retinoblastoma (Figure 2B). In contrast to the modest effects of *p16* inactivation in the *Rb/p107DKO* model, germline inactivation of a single allele of *Arf* led to rapid, usually bilateral, retinoblastoma (Figure 2, B and C). In the control *Rb/p107DKO* cohort, 6 out of 27 (22%) mice developed retinoblastoma (average time until visible tumor, 178 days). In contrast, 27 out of 33 (82%) of the *Rb/p107DKO;Arf*$^{+/-}$ mice developed retinoblastoma (average time until visible tumor, 151 days). Analyses of late-stage progression revealed a subset of late tumors that progressed to invade the brain (Figure 2C). Southern blot analyses revealed loss of heterozygosity (LOH) of the *Arf* allele in 13 out of 23 primary tumors and 2 out of 3 metastases (Figure 2D and data not shown). Most samples with *Arf* LOH showed complete loss of the *Arf* allele (Figure 2D). Rare cases of *Arf* LOH, in which some residual wild-type allele was present, reflect either the presence of wild-type contaminating cells in the tumor or *Arf* deletion in most but not all tumor cells. These studies reveal selection for *Arf* inactivation and show that *Arf* is a clear tumor suppressor in retinoblastoma.

Rb/p107/p53/Arf tumorigenesis analyses. Arf may suppress retinoblastoma through the canonical p53 pathway via inhibition of MDM2, or Arf may exert p53-independent effects. p53-independent functions of Arf have been revealed in other systems through observations of synergistic effects of combined *Arf* and *p53* mutation on tumorigenesis in mice (19). We generated *Rb/p107/p53* triple knockout (*Rb/p107/p53TKO*) animals, with or without heterozygous inactivation of *Arf*. *Rb/p107/p53TKO* mice developed rapid retinoblastoma (Figure 3A), similar to results previously reported (20). When we compared the time to late-stage retinoblastoma development in *Rb/p107/p53TKO* mice with that in *Rb/p107/p53TKO;Arf*$^{+/-}$ mice, we found no difference (Figure 3A). Our observation of frequent LOH of *Arf* in *Rb/p107DKO;Arf*$^{+/-}$ retinoblastomas provided a powerful means to test whether selection for *Arf* inactivation still occurs when the p53 pathway is disrupted. We isolated retinoblastomas from *Rb/p107/p53TKO;Arf*$^{+/-}$ animals and performed LOH analyses for *Arf* via Southern blot. We found that, in the absence of p53, 0 out of 13 retinoblastomas exhibited *Arf* LOH (Figure 3B). Thus, dele-

tion of *p53* completely abrogates the selective pressure to inactivate *Arf*. Moreover, we found no evidence that *Arf* functions in a *p53*-independent fashion to suppress retinoblastoma.

Direct p53 mutation in murine retinoblastomas. Despite the reported absence of *p53* mutation in human retinoblastomas (21, 22), the strong effect of *p53* loss in accelerating retinoblastoma in mice raised the possibility that *p53* might be directly mutated in murine retinoblastoma. Thus, we sequenced the region of *p53* subject to frequent mutation, exons 5 to 9 in *Rb/p107DKO* retinoblastomas. Three out of thirty-five retinoblastomas harbored direct *p53* mutations. Two were heterozygous R270H mutations, while the third was a heterozygous 4-bp frameshift mutation (Figure 3C). R270H corresponds to one of the most frequently mutated p53 sites in human tumors (R273H) and has been shown to exhibit dominant-negative and potential gain-of-function properties in mice (23, 24). This report is the first evidence to our knowledge of direct *p53* mutations in mouse retinoblastoma. Direct *p53* mutation was specific to murine retinoblastoma, as sequencing of exons 5 to 9 of a panel of 37 human retinoblastomas did not reveal *p53* mutations. Altogether, we observed *Arf* deletion, *MDM2* amplification, or direct *p53* mutation in approximately 28% of *Rb/p107DKO* murine retinoblastomas (Figure 3D). This provides genetic evidence that the *p53* pathway is important for suppressing retinoblastoma in mice. We did not find evidence of direct *p53* mutation in human retinoblastoma, in which focal alterations in known *p53* pathway components were less frequent (~11%) than in the murine model (Figure 3D).

p53 inactivation increases proliferation in Rb/p107DKO retina. Previous studies have demonstrated that inactivation of *p53* accelerates retinoblastoma in mice (7, 20), but there have been no in vivo analyses of early lesions to assess the nature of *p53* function that is important. To determine how *p53* loss promotes retinoblastoma, we compared the phenotype of *Rb/p107DKO* retinas with that of *Rb/p107/p53TKO* retinas. Examination of retinas at postnatal day (PND22) revealed that homozygous *p53* inactivation significantly increased proliferation in the *Rb/p107DKO* model, as assayed by both Ki67 and phospho-histone H3 staining (Figure 4, A and B). We also performed TUNEL staining to quantify apoptosis. We found that inactivation of p53 did not suppress apoptosis in the retina (Figure 4, A and B). Thus, our data support the notion that, even in the absence of *Rb*, a cell cycle block forms a barrier to retinoblastoma that is overcome through secondary genetic alterations.

With evidence that the p53 pathway engagement leads to cell cycle inhibition to prevent retinoblastoma, we investigated whether nonproliferative *Rb/p107DKO* retinas in older animals (~1 year) exhibited evidence of senescence. We performed senescence-associated β-galactosidase staining to examine senescence in retinas from *Rb/p107DKO* animals that lacked retinoblastoma. We found no senescence-associated β-galactosidase staining in control or *RB/p107DKO* nonproliferative retinas at 1 year of age (Supplemental Figure 5). Senescent cells typically exhibit a senescence-associated secretory phenotype (SASP), with increased expression of proinflammatory factors (25). We also examined SASP transcripts in control adult retinas, *Rb/p107DKO* nonproliferative retinas, and *Rb/p107/p53TKO* retinoblastomas (Supplemental Figure 6). Of the 8 SASP factors examined, only 1 (*Igfbp7*) was upregulated in the *Rb/p107DKO* retinas compared with control retinas. Despite upregulation of *Igfbp7* in *Rb/p107DKO* retinas, similar high levels remained in retinoblastomas that exhibited deletion of *p53*. Thus, the block to tumorigenesis that is overcome through *p53* mutation is distinct from a classical senescence response.

Discussion

It has been proposed that evasion of the *p53* pathway through *MDM4* amplification is important for retinoblastoma in humans (7). It is clear that strong overexpression of *MDM4* can promote retinoblastoma in mice (26), but our study reveals that most cases of increased *MDM4* copy number in human retinoblastoma arise through low-level gain of the whole long arm of 1q (Supplemental Figure 2). A novel mouse model that exhibits low levels of *MDM4* overexpression (27) will be an important tool to test the notion that low levels of increases in *MDM4* expression (i.e., via 1q gain) may be oncogenic in retinoblastoma. With a low frequency of focal, high-level *MDM4* amplifications in human retinoblastoma (2 out of 37 samples), we explored whether other components of the p53 pathway might be genetically altered in human retinoblastoma and mouse models. We report, for the first time to our knowledge, *p16INK4a/Arf* deletions in both human and murine retinoblastoma. Our mouse genetic analyses showed particularly strong tumor suppressive ability for *Arf* in a murine retinoblastoma model.

The strong effect of *Arf* loss in promoting murine retinoblastoma (Figure 2B) suggests that *Arf* is the major tumor suppressor in the large deleted region. *Arf* only appeared to be inactivated through deletions, as we found no *Arf*-specific mutations in retinoblastoma. Moreover, the *Arf* promoter is not silenced via methylation in human retinoblastoma (28). It is important to note that, in human and murine retinoblastomas with *Arf* deletion, the region of loss invariably included *p16INK4a* and *p15Ink4b* as well. *p16INK4a* loss alone led to a modest acceleration of *Rb/p107DKO* retinoblastoma (Figure 2A), and we have not investigated the possibility that co-mutation of *Arf* together with *p16INK4a* and/or *p15Ink4b* might exhibit cooperative effects in retinoblastoma suppression. Previous work indicated that upregulation of a number of CDK inhibitors (including p16Ink4a and p15Ink4b) occurs in response to *Rb/p107* deletion in the retina (14). Also, deletion of another CDKI, *Cdkn1a*, led to increased proliferation in the *Rb/p107DKO* retina in vivo (14). This result supports the notion that CDK inhibitors may act as tumor suppressors in the context of *RB* deletion. It will be interesting for future work to assess the roles of CDK inhibitors as retinoblastoma suppressors in the context of *Arf* mutation.

Arf has been shown to exhibit *p53*-independent activities in sperm development in mice (29). It has been hypothesized that *p53*-independent activities of *Arf* could contribute to the tumor suppressor function of *Arf* (reviewed in ref. 30). Indeed, mice lacking both *Arf* and *p53* develop a wider spectrum of tumors than that found in *Arf*-deficient or *p53*-deficient mice (19). We asked whether *p53* and *Arf* loss would synergize to promote retinoblastoma. We found no additive effect of *Arf* and *p53* codeletion on the incidence of murine retinoblastoma. Moreover, the absence of *p53* completely eliminated the selective pressure to inactivate the wild-type copy of *Arf*. Our data support the idea that *Arf* functions through the canonical *p53* pathway in retinoblastoma. We also report direct *p53* mutation and focal *MDM2* amplification in *Rb/p107DKO* murine retinoblastoma. Importantly, *Arf* deletion, *MDM2* amplification, and *p53* mutation were mutually exclusive in the murine tumors. Also, *MDM4* amplification and *CDKN2A*

deletion were not found in the same human retinoblastomas. Alterations in the same pathway at multiple levels across different tumors underscore the importance of this pathway in murine retinoblastoma models.

Human retinoblastoma has been proposed to arise from a benign lesion, termed retinoma (4). It was shown that retinoma, adjacent to normal retina and contiguous with malignant retinoblastoma, exhibited homozygous *RB* deletion but was nonproliferative (4). A limitation of human retinoma studies is that the lesions are studied in the presence of late-stage retinoblastoma that resulted in removal of the eye. The possibility that retinoma could represent a regressed region of retinoblastoma cannot be ruled out. Using mouse models, we could identify lesions that resembled murine retinoblastoma based on marker analyses but were nonproliferative. We hypothesize that murine retinoma-like lesions would have progressed to retinoblastoma had secondary mutations impaired the ability of the *Rb/p107DKO* cells to arrest/exit the cell cycle. Previous work has shown that many *Rb/p107DKO* cells can exit the cell cycle after an extended period of inappropriate proliferation during retinal development (5, 13) (also see Figure 4). In this study, we found that p53 deletion strongly promotes retinoblastoma, but without suppression of apoptosis (Figure 4). Instead, we found that p53 loss increased proliferation in the *Rb/p107DKO* retina. Thus, the proliferation machinery may need to be altered through multiple mutations in a single tumor, beyond *Rb* or *Rb/p107* mutation alone, for full disruption of the pathway. Recent studies investigating the *miR-17-92* microRNA cluster in retinoblastoma revealed that *miR-17-92* overexpression also promoted retinoblastoma via effects on proliferation control (14). Interestingly, suppression of p21Cip1 was implicated as conferring some of the effects of *miR-17-92*. As p21Cip1 is a known p53 target, it will be interesting for future work to assess whether p21Cip1 also plays a role in mediating the retinoblastoma-suppressing effects of p53. In human retinoblastoma, focal high-level amplification of *MDM4* or deletion of *CDKN2A* was relatively infrequent. We hypothesize that the ultimate effect of these alterations is a bypass of a proliferative block to tumorigenesis. Higher resolution analyses of the retinoblastoma genome may reveal additional mutated genes that act in the same pathway.

We have shown that the *CDKN2A* locus is deleted in a subset of murine and human retinoblastomas. We demonstrated that *Arf* exhibits potent tumor suppressor activity in mouse models and that the tumor-suppressing effects of *Arf* require *p53* to be intact. We found that p53 loss increases proliferation in the *Rb/p107DKO* retina without suppressing cell death. We believe that our study provides new insights into the *p53* pathway in retinoblastoma in humans and mice and demonstrates the importance of cooperation between *Rb* and *Arf* in tumor suppression.

Methods

Animals. *Rb/p107DKO* mice were bred with $p16^{-/-}$, $Arf^{-/-}$, or $p53^{lox/lox}$ strains to generate the compound mutant mice used in these studies. $Rb^{lox/lox}$ and $p107^{-/-}$ mice were from Tyler Jacks (Massachusetts Institute of Technology, Cambridge, Massachusetts, USA). $p16^{-/-}$, $Arf^{-/-}$, and $p53^{lox/lox}$ mice were obtained from the NCI MMHCC repository. These strains were originally generated by Ron Depinho, MD Anderson Cancer Center, Houston, Texas, USA ($p16^{-/-}$ *Cdkn2a* exon 1α deletion); Charles Sherr, St. Jude Children's Research Hospital, Memphis, Tennessee, USA ($Arf^{-/-}$ *Cdkn2a* exon 1β deletion); and Anton Berns, Netherlands Cancer Institute, Amsterdam, The Netherlands (*p53 lox*). Independent *Rb/p107DKO* cohorts were generated for the different crosses using breeding strategies that produced littermate *Rb/p107DKO* controls and *p16* or *Arf* mutant cohorts. Animals were maintained on a mixed genetic background. For tumor studies, animals were monitored visually for the presence of retinoblastoma that exhibited invasion into the anterior chamber of the eye.

Array-CGH. DNA was isolated from human and murine primary retinoblastomas using phenol-chloroform extractions. Murine array-CGH was performed using the ROMA platform, as described previously, using 84 K arrays (6, 31). Human retinoblastoma array-CGH was performed on 32 human retinoblastomas using custom Nimblegen 135 K arrays. The regions surrounding *CDKN2A* and *MDM4* were tiled a median distance of approximately 600 bp per probe, with a backbone spacing of 27 kb per probe through most of the genome. We also performed human ROMA analyses on an additional 5 human retinoblastomas using 84 K ROMA arrays.

Southern blot analyses. Genomic DNA was isolated from retinoblastoma or tail samples and digested with BglII. Standard Southern protocols were used, with an Arf exon 1β probe for hybridization, as described previously (32).

Immunoblot/immunohistochemistry/TUNEL analyses. Western blots were performed as described previously (14). For BrdU analyses, eyes were fixed in Bouin's solution overnight and processed through paraffin, and BrdU immunostaining was performed, as described previously (14). Immunohistochemistry and TUNEL were performed on eyes fixed in 4% paraformaldehyde as described previously (14). Antibodies used were as follows: Sox-2 (Santa Cruz Biotechnology Inc., Y-17), Syntaxin (Sigma-Aldrich), Arf (Abcam), Ki67 (Abcam), Active Caspase-3 (Cell Signaling Technology), Phospo-Histone H3 (Millipore), and BrdU (BD Biosciences). TUNEL assays were performed using the In Situ Death Detection Kit (Roche).

Real-time PCR. For expression analyses, RNA was isolated with TRIzol reagent (Invitrogen), and cDNAs were generated using SuperScript II (Invitrogen). SYBR green real-time PCR was performed using a DNA Engine Opticon (MJ Research). The ΔΔCT method was used. Primer sequences are shown in Supplemental Table 1.

p53 and CDKN2A sequencing. Exons 5 through 9 of murine and human *p53* and all exons of *CDKN2A* were PCR amplified. PCR products were sequenced using Sanger sequencing with the following primers for amplification and sequencing: murine *p53* exon 5 (forward 5′-TCTCTTCCAGTACTCTCCTC-3′, reverse 5′-GAGGGCTTACCATCACCATC-3′), exon 6 (forward 5′-TTGCTCTAAGGCCTGGCTCC-3′, reverse 5′-AATTACAGACCTCGGGTGGC-3′), exon 7 (forward 5′-TCTTCCCCAGGCCGGCTCTG-3′, reverse 5′-GCCTCCCTACCTGGAGTCTT-3′), exon 8 (forward 5′-TCCCGGATATGTGGGAACCTT-3′, reverse 5′-GCCTGCGTACCTCTCTTTGC-3′), and exon 9 (forward 5′-CCTTCCACAGCGCTGCCCAC-3′, reverse 5′-GCCTTGGTACCTTGAGGGTG-3′); murine *Cdkn2a* exon 1α (forward 5′-CAGGTCAGGAGCAGAGTGTG-3′, reverse 5′-GCAGCAGCAACAACAAAAAC-3′), exon 1β (forward 5′-CTTCTCACCTCGCTTGTCAC-3′, reverse 5′-ACCGTGTGCAAAGTACTCCA-3′), exon 2 (forward 5′-AGCCTCCTGACTGTGGATGT-3′, reverse 5′-GACTGAGAGGCTGCAAAACC-3′), and exon 3 (forward 5′-TGGCACCTAGGACAGCTTTA-3′, reverse 5′-TGAGAGTTTGGGGACAGAGG-3′); and human *CDKN2A* exon 1α (forward 5′-AGTGAACGCACTCAAACACG-3′, reverse 5′-GGCCTCCGACCGTAACTATT-3′), exon 1β (forward 5′-GTCCCAGTCTGCAGTTAAGG, reverse 5′-AGTCGTTGTAACCCGAATGG-3′), exon 2 (forward 5′-GGAAATTGGAAACTG GAAGC-3′, reverse 5′-TCTGAGCTTTGGAAGCTCT-3′), and exon 3 (forward 5′-TGCCACACATCTTTGACCTC-3′, reverse 5′-CGATCTTGAGACACGGCTTT-3′). Primer sequences for amplification and sequencing of human p53 exons 5 through 9 were previously described (33).

Senescence assays. Senescence-associated β-galactosidase staining was performed on fresh frozen retinas and control kidney tissue, as described previously (34). Briefly, 10-μm slides were fixed for 10 minutes in 4% PFA in PBS, washed with PBS, and stained for 14 hours in stain solution (pH 6.0). Slides were counterstained with eosin.

Statistics. Two-tailed Student's *t* test was used for comparisons of different groups. A *P* value of less than 0.05 was considered significant. Error bars correspond to standard deviation.

Study approval. All protocols that used human retinoblastoma material were approved by both the Johns Hopkins Homewood Institutional Review Board (Baltimore, Maryland, USA) and the Massachusetts Eye and Ear Infirmary Human Studies Committee (Boston, Massachusetts, USA). All protocols involving mice were approved by the Carnegie Institution Animal Care and Use Committee (Baltimore, Maryland, USA).

Acknowledgments

The authors thank Tyler Jacks, Charles Sherr, Anton Berns, Ron Depinho, and Peter Gruss for providing valuable mouse strains used in these studies. The laboratory of D. MacPherson is supported by grant R01 5R01CA148867 from the NCI/NIH. S. Mukai received support from the Mukai Fund.

Received for publication October 19, 2011, and accepted in revised form February 22, 2012.

Address correspondence to: David MacPherson, Department of Embryology, Carnegie Institution, 3520 San Martin Drive, Baltimore, Maryland 21218, USA. Phone: 410.246.3084; Fax: 410.243.6311; E-mail: macpherson@ciwemb.edu.

1. Macpherson D. Insights from mouse models into human retinoblastoma. *Cell Div*. 2008;3:9.
2. Corson TW, Gallie BL. One hit, two hits, three hits, more? Genomic changes in the development of retinoblastoma. *Genes Chromosomes Cancer*. 2007; 46(7):617–634.
3. Burkhart DL, Sage J. Cellular mechanisms of tumour suppression by the retinoblastoma gene. *Nat Rev Cancer*. 2008;8(9):671–682.
4. Dimaras H, et al. Loss of RB1 induces non-proliferative retinoma; increasing genomic instability correlates with progression to retinoblastoma. *Hum Mol Genet*. 2008;17(10):1363–1372.
5. Chen D, Livne-bar I, Vanderluit JL, Slack RS, Agochiya M, Bremner R. Cell-specific effects of RB or RB/p107 loss on retinal development implicate an intrinsically death-resistant cell-of-origin in retinoblastoma. *Cancer Cell*. 2004;5(6):539–551.
6. MacPherson D, Conkrite K, Tam M, Mukai S, Mu D, Jacks T. Murine bilateral retinoblastoma exhibiting rapid-onset, metastatic progression and N-myc gene amplification. *EMBO J*. 2007;26(3):784–794.
7. Laurie NA, et al. Inactivation of the p53 pathway in retinoblastoma. *Nature*. 2006;444(7115):61–66.
8. Xu XL, et al. Retinoblastoma has properties of a cone precursor tumor and depends upon cone-specific MDM2 signaling. *Cell*. 2009;137(6):1018–1031.
9. Aslanian A, Iaquinta PJ, Verona R, Lees JA. Repression of the Arf tumor suppressor by E2F3 is required for normal cell cycle kinetics. *Genes Dev*. 2004; 18(12):1413–1422.
10. Bates S, et al. p14ARF links the tumour suppressors RB and p53. *Nature*. 1998;395(6698):124–125.
11. Brennan RC, et al. Targeting the p53 Pathway in Retinoblastoma with Subconjunctival Nutlin-3a. *Cancer Res*. 2011;71(12):4205–4213.
12. Marquardt T, Ashery-Padan R, Andrejewski N, Scardigli R, Guillemot F, Gruss P. Pax6 is required for the multipotent state of retinal progenitor cells. *Cell*. 2001;105(1):43–55.
13. MacPherson D, Sage J, Kim T, Ho D, McLaughlin ME, Jacks T. Cell type-specific effects of Rb deletion in the murine retina. *Genes Dev*. 2004; 18(14):1681–1694.
14. Conkrite K, et al. miR-17~92 cooperates with RB pathway mutations to promote retinoblastoma. *Genes Dev*. 2011;25(16):1734–1745.
15. Lowe SW, Sherr CJ. Tumor suppression by Ink4a-Arf: progress and puzzles. *Curr Opin Genet Dev*. 2003; 13(1):77–83.
16. Sharpless NE, DePinho RA. The INK4A/ARF locus and its two gene products. *Curr Opin Genet Dev*. 1999; 9(1):22–30.
17. Sangwan M, et al. Established and new mouse models reveal E2f1 and Cdk2 dependency of retinoblastoma, and expose effective strategies to block tumor initiation [published online ahead of print January 30, 2012]. *Oncogene*. doi:10.1038/onc.2011.654.
18. McKeller RN, et al. The Arf tumor suppressor gene promotes hyaloid vascular regression during mouse eye development. *Proc Natl Acad Sci U S A*. 2002;99(6):3848–3853.
19. Weber JD, et al. p53-independent functions of the p19(ARF) tumor suppressor. *Genes Dev*. 2000; 14(18):2358–2365.
20. Zhang J, Schweers B, Dyer MA. The first knockout mouse model of retinoblastoma. *Cell Cycle*. 2004; 3(7):952–959.
21. Gallie BL, Campbell C, Devlin H, Duckett A, Squire JA. Developmental basis of retinal-specific induction of cancer by RB mutation. *Cancer Res*. 1999; 59(7 suppl):1731s–1735s.
22. Kato MV, et al. Loss of heterozygosity on chromosome 17 and mutation of the p53 gene in retinoblastoma. *Cancer Lett*. 1996;106(1):75–82.
23. Olive KP, et al. Mutant p53 gain of function in two mouse models of Li-Fraumeni syndrome. *Cell*. 2004; 119(6):847–860.
24. de Vries A, et al. Targeted point mutations of p53 lead to dominant-negative inhibition of wild-type p53 function. *Proc Natl Acad Sci U S A*. 2002; 99(5):2948–2953.
25. Coppe JP, Desprez PY, Krtolica A, Campisi J. The senescence-associated secretory phenotype: the dark side of tumor suppression. *Annu Rev Pathol*. 2010; 5:99–118.
26. McEvoy J, et al. Coexpression of normally incompatible developmental pathways in retinoblastoma genesis. *Cancer Cell*. 2011;20(2):260–275.
27. De Clercq S, et al. Widespread overexpression of epitope-tagged Mdm4 does not accelerate tumor formation in vivo. *Mol Cell Biol*. 2010;30(22):5394–5405.
28. Choy KW, Pang CP, To KF, Yu CB, Ng JS, Lam DS. Impaired expression and promotor hypermethylation of O6-methylguanine-DNA methyltransferase in retinoblastoma tissues. *Invest Ophthalmol Vis Sci*. 2002;43(5):1344–1349.
29. Churchman ML, Roig I, Jasin M, Keeney S, Sherr CJ. Expression of arf tumor suppressor in spermatogonia facilitates meiotic progression in male germ cells. *PLoS Genet*. 2011;7(7):e1002157.
30. Sherr CJ. Divorcing ARF and p53: an unsettled case. *Nat Rev Cancer*. 2006;6(9):663–673.
31. Lakshmi B, et al. Mouse genomic representational oligonucleotide microarray analysis: detection of copy number variations in normal and tumor specimens. *Proc Natl Acad Sci U S A*. 2006; 103(30):11234–11239.
32. Tsai KY, et al. ARF mutation accelerates pituitary tumor development in $Rb^{+/-}$ mice. *Proc Natl Acad Sci U S A*. 2002;99(26):16865–16870.
33. Liu Y, Bodmer WF. Analysis of P53 mutations and their expression in 56 colorectal cancer cell lines. *Proc Natl Acad Sci U S A*. 2006;103(4):976–981.
34. Debacq-Chainiaux F, Erusalimsky JD, Campisi J, Toussaint O. Protocols to detect senescence-associated beta-galactosidase (SA-betagal) activity, a biomarker of senescent cells in culture and in vivo. *Nat Protoc*. 2009;4(12):1798–1806.